Journal Pre-proof

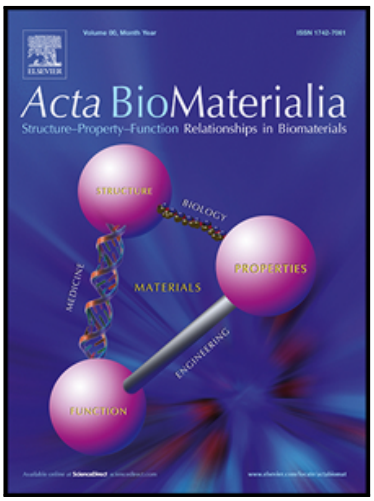

Human tendon-derived cell sheets created by magnetic force-based tissue engineering hold tenogenic and immunomodulatory potential

Adriana Vinhas , Ana I. Gonçalves , Márcia T. Rodrigues , Manuela E. Gomes

PII: S1742-7061(21)00410-4
DOI: https://doi.org/10.1016/j.actbio.2021.06.036
Reference: ACTBIO 7450

To appear in: *Acta Biomaterialia*

Received date: 19 March 2021
Revised date: 14 June 2021
Accepted date: 22 June 2021

Please cite this article as: Adriana Vinhas , Ana I. Gonçalves , Márcia T. Rodrigues , Manuela E. Gomes , Human tendon-derived cell sheets created by magnetic force-based tissue engineering hold tenogenic and immunomodulatory potential, *Acta Biomaterialia* (2021), doi: https://doi.org/10.1016/j.actbio.2021.06.036

Human tendon-derived cell sheets created by magnetic force-based tissue engineering hold tenogenic and immunomodulatory potential

Adriana Vinhas [a,b #], Ana I. Gonçalves [a,b #], Márcia T. Rodrigues [a,b], Manuela E. Gomes [a,b *]

[a]3B's Research Group, I3Bs - Research Institute on Biomaterials, Biodegradables and Biomimetics, University of Minho, Headquarters of the European Institute of Excellence on Tissue Engineering and Regenerative Medicine, Avepark - Zona Industrial da Gandra, 4805-017 Barco, Guimarães, Portugal
[b]ICVS/3B's - PT Government Associate Laboratory, Braga/Guimarães, Portugal

# Equally contributed

*Corresponding Author: Manuela E. Gomes. e-mail: megomes@i3bs.uminho.pt.

Keywords: Tendon derived cells, magnetic nanoparticles, magnetic cell sheets, inflammation

Abstract

Cell sheet technology and magnetic based tissue engineering hold the potential to become instrumental in developing magnetically responsive living tissues analogues that can be potentially used both for modelling and therapeutical purposes. Cell sheet constructions more closely recreate physiological niches, through the preservation of contiguous cells and cell-ECM interactions, which assist the cellular guidance in regenerative processes.

We herein propose to use magnetically assisted cell sheets (magCSs) constructed with human tendon-derived cells (hTDCs) and magnetic nanoparticles to study inflammation activity upon magCSs exposure to IL-1β, anticipating its added value for tendon disease modelling.

Our results show that IL-1β induces an inflammatory profile in magCSs, supporting its *in vitro* use to enlighten inflammation mediated events in tendon cells. Moreover, the response of magCSs to IL-1β is modulated by pulsed electromagnetic field (PEMF) stimulation,

favoring the expression of anti-inflammatory genes, which seems to be associated to MAPK(ERK1/2) pathway. The anti-inflammatory response to PEMF together with the immunomodulatory potential of magCSs opens new perspectives for their applicability on tendon regeneration that goes beyond advanced cell based modelling.

1. Introduction

Cell sheet technology introduces the possibility of providing stable cellular constructs and thus enabling the construction of tissue-like assemblies [1]. In fact, cell sheets (CSs) preserve structural elements as ion channels, growth factor receptors, and cell surface proteins as well as intercellular connections and matrix components, which assist cell sheet usefulness either as biomimetic models to address tissue functional aspects or as tissue substitutes. Previous studies reported cell sheet potential to stimulate musculoskeletal tissue regeneration [2, 3]. Furthermore, mesenchymal stem cell sheets demonstrated a satisfactory integration into native tissues accompanied by anti-inflammatory effects improving cartilage repair and treatment of osteoarthritis disease[4, 5]. With inflammation increasingly recognized as a central component both in healing and in disease progression, a model to study inflammation in tendon tissues taking advantage of CSs technology could become an important tool to advance knowledge in this field. For instance, it has been reported that adipose tissue derived stem cells (ASC) sheets improve matrix remodelling, and modulate the inflammatory phase facilitating tendon healing [6].

Magnetic cell sheets were constructed by magnetic force-based TE (Mag-TE) as firstly proposed by Ito A. *et al* in 2004 [7], and described by our group [2]. Specifically, this

methodology uses magnetite nanoparticles and magnetic force to construct magnetic sheets. As so, a confluent monolayer of cells is combined with MNPs and cultured under a permanent magnet. MagCSs offer the opportunity to study inflammatory cues and cell responses through contact-free stimulation of tendon resident cells in a more tissue-like environment with intercellular signaling and structural complexity [5, 8]. Also, magnetic cell sheets technology has demonstrated promising results in vascular [9, 10], cardiac[11] and musculoskeletal [2, 12, 13] tissue engineering strategies, however, very few examples were provided in the literature of magnetic cell sheets in therapies for resolving inflammation. Our group has previously shown that magCSs exhibited a tendon-like ECM, good mechanoelastic properties and responsiveness, suggesting the applicability of these living patches in tendon therapies [2].

Moreover, magCSs could also enable to insight on pulsed electromagnetic field (PEMF) assisted immunomodulatory effects in cell-based therapies for functional tendon tissue replacement.

A controlled pro-inflammatory milieu can be provided to magnetic tendon cell sheets by the exogenous supplementation of interleukin-1β (IL-1β) to the culture medium. IL-1β is a pro-inflammatory cytokine released in inflammatory environments [14] and a well described marker of chronic inflammation [15, 16]. From previous reports by our group [17, 18] and others [19-21] exposure to low frequency (2 to 75Hz) and low strength (1.5 to 82mT) magnetic fields, was shown to modulate tendon cell response to inflammation stresses influencing the release and expression of cytokines [17, 18]. Other works also showed the effectiveness of the combination of magnetic nanoparticles (MNPs) with magnetic field for pain control and enhanced functional recovery in the knee diseases and osteoarthritic lesions [22]. Moreover, it has been reported by Rahmi et al. [23] that bone marrow-derived mesenchymal stem cell sheets labelled with MNPs upregulated anti-inflammatory factors,

TGF-β2 and IL-10, which increased the potential of magnetic cell sheets for therapeutic strategies.

In this work, we aimed at using magnetic cell sheet technologies to study tendon cell responses in inflammatory environments, induced by exposure of the cell sheets to IL-1β. We propose magCSs as a pathophysiological model of inflammation to more closely study the onset of tendon lesions and the inflammatory molecules affecting injured tendons, taking advantage of magCSs properties over cell monolayers. Furthermore, as PEMF favors anti-inflammatory cell responses, we also studied the role of magCSs assisted by a remote PEMF in IL-1β induced tendon cells responses.

2. Materials and Methods

2.1. Isolation and culture of human tendon derived cells (hTDCs)

hTDCs were isolated from surplus healthy tissue samples of patellar tendons, collected from adult patients undergoing orthopedic reconstructive surgeries under protocols previously established with Hospital da Prelada (Porto, Portugal) and with informed consent of the patients. The content of the written informed consent and related procedures were reviewed and approved by the Hospital Ethics Committee (P.I. N.º005/2019). The tendon tissue identification and quality (healthy/diseased) was assessed by the medical team during surgical intervention.

Following a previously established protocol [24-26], tendon samples were minced using a sterile scalpel. PBS drops were added in a continuous basis to keep a moist environment and reduce cell damage by mechanical forces. The excess of PBS was removed using a filtration system for 50 ml tubes (Falcon). Minced samples were collected into a 50 mL tube (Falcon), already containing an enzymatic solution of collagenase (0.1%, Sigma-Aldrich, C6885, USA) with 2M CaCl2 (1:1000, VWR, Germany) and 1% bovine serum albumin (BSA) (Sigma-

Aldrich, USA) for 1h at 37˚C under constant agitation. A ratio of 1:1 of minced tissue to the enzymatic solution was considered. After incubation, digested samples were filtered and centrifuged three times at 290 g for 5 min, and the supernatant discarded. Isolated hTDCs were expanded in α-MEM medium (A-MEM, Invitrogen, Life Technologies Limited, Paisley, UK) composed of α-MEM supplemented with 10% fetal bovine serum (FBS) (Alfagene, Life Technologies Limited, UK) and 1% antibiotic/antimicotic solution (A/A) (Alfagene, Life Technologies Limited, UK) in humidified 5% CO_2 atmosphere. hTDCs from passage 1 to 3 were used to perform all the experiments.

2.2. Magnetic cell sheets construction, culture, and stimulation

Magnetic cell sheets (magCSs) were constructed as previously described by our group.[2] Briefly, hTDCs were seeded onto 24-well tissue culture plates (BD Biosciences, San Jose UK) at a density of 500,000 cells per well. Two hours after seeding, the chitosan coated iron oxide MNPs (nanomag-C, 04-00-152, Micromod, Germany) were added to adherent hTDCs at 200 pg/cell. Then, MNPs were overnight incubated with the cells in α-MEM medium (A-MEM, Invitrogen, Life Technologies Limited, Paisley, UK) on a 24-well permanent magnet well-array plate (magnetic induction of 350mT per magnet per well) in humidified 5% CO_2 atmosphere.

Then, 16h after MNPs addition, magCSs were washed with D-PBS (Sigma-Aldrich, Saint Louis, MO) and the culture medium replaced by either *i)* α-MEM medium (magCSs Control group) or *ii)* α-MEM medium supplemented with IL-1β (1 ng/mL, Alfagene, Life Technologies Limited, UK) for 24 hours (magCSs IL-1β group) to induce inflammatory cues in hTDCs, as previously established [17]. To assess the immunomodulatory effect of PEMF, 24h after supplementation with IL-1β magCSs were stimulated with PEMF (magCSs IL-1β PEMF group) using a magnetotherapy device (Magnum XL Pro; Globus Corporation, Italy) for 1 hour in humidified 5% CO_2 atmosphere. The magCSs were placed between two coils

(solenoids) and the magnetic field was generated by the electric current that goes through a coil. The stimulus provided was selected from a set of therapeutic programs used in health-rehab medical treatments.

These treatments typically range between 10 min and 12 hours and the parameters of magnetic fields are between 5 to 200Hz, and strength 0.2 to 10mT.

These parameters are known to be safe and with therapeutic value in humans. Having this in mind, together with the outcomes from previous studies of our group with tendon cell cultures, the PEMF parameters of 5 Hz of frequency, 4 mT of intensity and 50 % duty cycle were established as optimal parameters for modulating inflammatory cues [17]. Moreover, in these studies we also determined the 1h exposure period as suffice to elicit a desirable response in IL-1β primed tendon cells either cultured in monolayer (Vinhas, A. et al, 2020a) or in magnetic-responsive systems (Vinhas, A. et al, 2020b).

In sum, the following conditions were investigated: i) magCSs in α-MEM medium (Control), ii) IL-1β-treated magCSs (IL1-β), iii) IL-1β-treated magCSs exposed to PEMF (IL1-β PEMF). Magnetic cell sheets were characterized at day 3 (counting from tendon cell seeding on the plates) for cell viability, proliferation and morphological analysis. Matrix deposition, collagen production, and gene expression levels of tendon and inflammatory markers were also investigated. Additionally, the culture media of magCSs was collected and the presence of inflammatory mediators quantified using ELISA assays.

2.3. Cell distribution and matrix deposition - tendon cell monolayers vs magCSs constructions

A Hematoxylin & Eosin (HE) stain was performed for comparative analysis of the distribution of cells in tendon cell monolayer and magCSs constructions. Thus, tendon cell monolayers and magCSs (control condition), both seeded at 500,000 cells/well and cultured

for 3 days were stained using Hematoxylin (7211, Thermo Scientific) and Eosin-Y Alcoholic solution (71204, Thermo Scientific) for cytoplasmic detection.

To confirm the stability of magCSs and matrix deposition in magCSs and in tendon cell monolayer, Sirius Red/Fast Green Collagen Staining Kit (9046, Chondrex) was performed for a qualitative analysis. magCSs and tendon cell monolayers were fixed with a 10% (v/v) neutral buffered formalin solution (Bio Optica, Milano, Italy). Then the dye solution from the kit was added to the magCSs and to the cells in monolayer followed by 40 min incubation.

HE and Sirius Red/Fast Green stained samples were visualized and images obtained using a fluorescence inverted microscope (Axio Observer, Zeiss, Göttingen, Germany).

Immunostaining for collagen I was also performed as detailed described in section **2.9.**

2.4. Assessment of cellular viability and cell proliferation

Live/dead assay was performed to assess cellular viability. Briefly, the magCSs were incubated for 20 min with calcein-AM (2 μg/ml) and propidium iodide (3 μg/ml), both from Life Technologies Limited, UK. Afterwards, cells were washed with PBS and visualized under a fluorescence inverted microscope (Axio Observer, ZEISS, Germany).

The cell viability of magCSs was evaluated by MTS assay (Cell Titer 96 Aqueous Solution Cell Proliferation Assay, Promega). MagCSs were washed in PBS before a 3h incubation in a mixture of phenol red free medium supplemented with FBS and MTS solution (5:1 ratio) at 37 ºC and 5% CO_2 atmosphere, protected from light. Then, the supernatant was transferred to a new 96-well plate and the absorbance read at 490 nm (Synergy^{TM}HT, BIO-TEK Instruments, Winooski, Vermont). Triplicates were made of each sample and a blank sample (no cells) reading was performed.

The cell proliferation of magCSs constructions were evaluated by Quant-It PicoGreen dsDNA assay Kit (Thermo Fisher Scientific). magCSs from all conditions were washed with

PBS, transferred to a microtube with 1ml of sterile ultrapure water and kept at -80ºC until analysis. Samples were thawed, sonicated and processed according to the manufacturer's instructions, at an excitation/emission wavelength of 485/528nm (Synergy^{TM}HT, BIO-TEK Instruments, Winooski, Vermont). Samples and standards were made in triplicate.

2.5. Morphological characterization

The morphological characterization of the magCSs was analyzed by scanning electron microscopy (Auriga Compact, ZEISS, Germany). The elementary composition of magCSs was also investigated by Energy dispersive x-ray spectroscopy (EDS) (JSM-6010LV, JEOL, Japan) to confirm the presence of iron (Fe) element within magCSs constructions. For this purpose, the magCSs were fixed in 10% (v/v) neutral buffered formalin for 1 h at room temperature and dehydrated in a series of increasing ethanol solutions (from 30% to 100% (v/v)), followed by a 5min immersion in hexamethyldisiloxane (HMSO, Sigma-Aldrich, Saint Louis, MO, USA). Subsequently, the samples were air-dried overnight and sputter coated with gold (30s at 20mA, Cressington, C5219, Model 108A).

2.6. Gene expression evaluation by RT-PCR

The expression of tenogenic markers, namely Mohawk *(MKX),* Scleraxis *(SCX),* Tenomodulin *(TNMD),* Decorin *(DCN),* Metalloproteinase-1 *(MMP-1),* Metalloproteinase-2 *(MMP-2),* Metalloproteinase-3 *(MMP-3),* Inhibitor of Metalloproteinase-1 *(TIMP-1),* Collagen type I *(COL1A1),* Collagen type III *(COL3A1),* and inflammation markers, namely Interleukin-8 *(IL-8),* Interleukin-1β *(IL-1β),* Tumor necrosis factor *(TNFα),* Interleukin-6 *(IL-6),* Interleukin-10 *(IL-10),* Interleukin-4 *(IL-4),* was assessed by real time RT-PCR.

Total RNA was extracted from all samples under study, using TRI reagent (T9424, Sigma-Aldrich, Saint Louis, MO, USA) according to the manufacturer's instructions. Briefly, TRI reagent was added to each sample and stored at -80°C. After defrosting, samples were

incubated with chloroform (Sigma-Aldrich, Saint Louis, MO, USA) for 15 min and centrifuged at 12,000 g for 15 min at 4°C. The aqueous fraction was collected and isopropanol (Sigma-Aldrich, Saint Louis, MO, USA) was added. After 10 min, samples were centrifuged at 12,000 g for 10 min at 4°C. RNA pellet was washed with ethanol (70% v/v) and subsequently centrifuged at 7,500 g for 5 min at 4°C. RNA quantity and purity were determined with a NanoDrop ND-1000 spectrophotometer (Wilmington, DE, USA). The cDNA synthesis was performed using the qScript cDNA Synthesis kit (qScript^{TM} cDNA Synthesis Kit, Quanta Biosciences, Gaithersburg, MD, USA) in a Mastercycler Realplex (Eppendorf, Hamburg, Germany). An initial amount of total RNA of 1 µg in a total volume of 20 µL was used per each and every sample. The quantification of the transcripts was carried out by quantitative polymerase chain reaction (qPCR) using the PerfeCTA SYBR Green FastMix kit (Quanta Biosciences, Gaithersburg, MD, USA) following the manufacturer's protocol, in a Real-Time Mastercycler Realplex thermocycler (Eppendorf, Hamburg, Germany).

The primers were pre-designed with PerlPrimer v1.1.21 software (Supplementary Table S1) and synthesized by MWG Biotech. *GAPDH* was used as the housekeeping gene. The $2^{-\Delta\Delta Ct}$ method was selected to evaluate the relative expression level for each target gene. All values were firstly normalized against *GAPDH* expression values, and then to magCSs cultured in α-MEM medium at day 3.

2.7. Quantification of secreted forms of inflammatory mediators

The release of inflammatory mediators was analysed from cell supernatants of all magCSs conditions. The supernatants were tested using commercially available enzyme immunoassay kits for TNFα (Human TNFα ELISA Kit, EK0525, Tebu-Bio, Fremont, CA, USA), COX-2 (Human COX-2 ELISA Kit, KA0323, Abnova, Taiwan), PGE_2 (Human Prostaglandin E2 ELISA Kit, KHL1701, Thermo Fisher Scientific, Molecular Probes, Eugene, USA), IL-6

(Human IL-6 Standard ABTS ELISA Development Kit, 900-K16, Peprotech, Rocky Hill, NJ, USA), and IL-10 (Human IL-10 Standard ABTS ELISA Development Kit, 900-K21; Peprotech, Rocky Hill, NJ, USA). MAPK protein phosphorylation was also determined in cytoplasmic protein extracts using the PhosphoTracer ERK1/2 (pT202/Y204)+p38 MAPK (pT180/Y182)+JNK1/2/3 (pT183/Y185) Elisa Kit (Abcam, ab119674, Cambridge, UK). Each and every kit were performed following the manufacturers' instructions.

2.8. Quantification of extracellular matrix proteins

The amount of collagen and non-collagenous proteins was determined using a semiquantitative assay, namely Sirius Red/Fast Green Collagen Staining Kit (9046, Chondrex). For this purpose, samples of all magCSs conditions were fixed with a neutral buffered formalin solution and stored at 4 °C until analysis. Then the dye solution from the kit was added to the magCSs followed by 40 min incubation. A dye extraction buffer was then mixed and the OD values read in a spectrophotometer (Synergy HT, Biotek Instruments) at 540 nm and 605 nm. The results of collagen and non-collagenous proteins were normalized to dsDNA quantified in section **2.4**.

2.9. Evaluation of tenogenic markers in magCSs constructions

Protein expression of Mohawk, Tenomodulin and Collagen type I was assessed by immunocytochemistry for all magCSs conditions in study. magCSs were washed three times with PBS, before and after fixation with 10% (v/v) neutral buffered formalin overnight and kept in PBS at 4°C until usage. Subsequently, the cells were incubated with 0.025% Triton-X100 in PBS solution (Sigma-Aldrich, Saint Louis, MO) and the blocking step was performed using Normal Horse Serum (Ready To Use Vectastain Kit, PK-7200; Vector, California). The magCSs were incubated overnight with anti-MKX (Rabbit anti-human, A83377, 1:100, Sigma-Aldrich, Saint Louis, MO), anti-Tenomodulin (Rabbit anti-human,

ab81328, 1:100, Abcam, Cambridge, UK), anti-Collagen type I (Rabbit anti-human, ab34710, 1:100, Abcam, Cambridge, UK) diluted in antibody diluent with background reducing components (Dako, Santa Clara, CA) at 4°C, followed by 1 h incubation at room temperature with the secondary antibody (donkey anti-rabbit Alexa Fluor 488, 1:200; Alfagene, Life Technologies Limited, UK). The samples were washed three times with PBS and stained with 4′,6-diamidino-2-phenyindole, dilactate (DAPI, 5 μg/μl, D9564; Sigma-Aldrich, Saint Louis, MO) for 10 min.

The immunostained samples were then analyzed by confocal laser scanning microscopy (CLSM, TCS SP8, Leica, Wetzlar, Germany). Images were bidirectionally scanned at 400 Hz with Argon (488) and UV (405) lasers and acquired using a 63x magnification objective. Three independent experiments were investigated for protein detection by immunofluorescence.

2.10. Assessment of nuclei elongation ratio

Nuclei aspect ratio was determined measuring a minimum of 30 nuclei of confocal microscopy images obtained in section **2.9**. Nuclei were imaged in different regions of magCSs samples. All three magCSs conditions were analysed using ImageJ software (version 1.52d). The ratio was defined by length was divided by the width to obtain the correspondent nuclei elongation ratio.

2.11. Western Blotting

The MAPK protein phosphorylation was also investigated by western blotting assay. magCSs were collected in PBS, resuspended, and the supernatant collected to a new microtube upon magnetic separation (MPC®-S, Dynal Biotech).

The total cell lysates were prepared using RIPA buffer (Sigma-Aldrich, Saint Louis, MO) with protease inhibitor cocktail (Sigma-Aldrich, Saint Louis, MO) and phosSTOP (ROCHE, Switzerland, EU). The samples were centrifuged for 15 min at 21, 952 g at 4°C and the supernatants collected. Afterwards, the BCA protein assay kit (Alfagene, Life Technologies Limited, UK) was used to assess the protein content of the samples according to the manufacturer's instructions. The protein extracts were resolved in 10% sodium dodecyl sulfate-polyacrylamide gels, followed by semi-dry transfer to Amersham™ Protran® Western blotting membranes (nitrocellulose; Sigma-Aldrich, Saint Louis, MO). The transfer of the proteins to the membrane was performed in a Pierce Power Station (Thermo Fisher Scientific, Molecular Probes, Eugene, OR). The membranes were blocked with 5% BSA in Tris-buffered saline with Tween 20 (Sigma-Aldrich, Saint Louis, MO) (TBS-T) and incubated with rabbit anti-phospho-p44/42 MAPK (Erk1/2) (1:1000) (9102; Cell signaling Technology, Danvers, MA), anti-collagen III (1:1000) (ab184993; Abcam, UK), anti-Tenomodulin (1:1000) (ab184993; Abcam, UK), anti-MKX (1:1000) (HPA006927; Sigma-Aldrich, Saint Louis, MO) and anti-α smooth muscle actin (1:2000) (ab32575; Abcam, UK) antibodies for 1h at room temperature under mild agitation. The membranes were washed three times with TBS-T and then incubated with a secondary antibody (1:2000) (Anti-Rabbit IgG Alkaline Phosphatase antibody, A9919, Sigma-Aldrich, Saint Louis, MO) for 1h at RT. A colorimetric AP substrate reagent kit (1706432; BioRad, Hercules CA) was used for color development. Semi-quantitative analysis was performed for pMAPK bands using ImageJ software (version 1.52d). α-actin was used as an internal control and for normalization of bands measurements.

2.12. Statistical analysis

Results are expressed as mean ± standard error of the mean (SEM). The statistical analysis was performed using GraphPad Prism6 software. Data was obtained from 3-independent experiments (n=3) analyzed in triplicate, and evaluated by Two-way ANOVA followed by Bonferroni post-hoc test for multiple comparison tests.

Symbols denote a different degree of confidence, * $p < 0.05$, ** $p < 0.01$, *** $p < 0.001$ and **** $p < 0.0001$.

3. Results

3.1. Improved tendon cell organization and matrix production in magCSs constructions

HE stain was performed to infer on the cellular distribution of magCSs in comparison to a simple tendon cell monolayer. A hyperdense culture was observed in both cultures (Fig. 1A, 1B) however cells in tendon cell monolayer are more randomly distributed. Also, magCSs evidence a higher level of spatial organization.

Sirius red/Fast green staining together with collagen I confirmed matrix deposition by tendon cells, which is more abundant and richer in collagen I in magCSs constructions (Fig. 1Aii, Bii).

3.2. Assessment of viability, cell content and micro-morphology in magCSs constructs

The MTS and Live/Dead assays were performed to confirm the non-cytotoxic effect of MNPs on tendon cells. High cell viability outcomes were verified in all conditions studied

demonstrating the suitability of the MNPs concentration applied and of magCSs constructions for in vitro cell based approaches (Fig. 2Ai, 2Aii).

In terms of dsDNA content (Fig. 2Aiii), IL-1β-magCSs under PEMF showed the higher dsDNA concentration among all conditions studied ($p<0.05$).

In tendon tissues cell nuclei and overall cell morphology follows an elongated shape. Elongated nuclei display ratio superior to 1, and, the average aspect nuclei ratio in IL-1β-magCSs under PEMF showed the highest values (>1) among the conditions studied (Fig. 2Aiv) ($p<0.0001$ in comparison to control group and $p<0.0001$ to IL-1β-magCSs). Moreover, IL-1β-magCSs showed the lowest nuclei aspect ratio ($p<0.05$ to control group and $p<0.0001$ to IL-1β-magCSs under PEMF). This result suggests that PEMF favors an elongated shape nucleus, and that IL-1β rich environments influence a more rounded shaped nucleus.

SEM analysis (Fig. 2B) also supports a tendency for the alignment distribution of magCSs within different layers of cells suggesting the establishment of intercellular connections among cells.

3.3. Tenogenic phenotype in magCSs under an IL-1β rich environment

The impact of IL-1β supplementation and PEMF exposure was evaluated on the tendon markers expressed by magCSs to assess their influence on the maintenance of tenogenic profile. With an exception for *SCX*, the relative expression of *MKX*, *TNMD*, and *DCN* were significantly affected by the IL-1β treatment [19, 27, 28] (Fig. 3).

MKX and *DCN* show a significant decrease in the expression values in comparison to Control and IL-1β PEMF groups ($p<0.05$) (Fig. 3A), while *TNMD* levels tend to decrease with both PEMF stimulation ($p<0.01$ to Control) and IL-1β treatment ($p<0.0001$ to Control group) (Fig. 3A). *SCX* expression seems not to be affected by IL-1β treatment or PEMF, showing similar values for all conditions studied (Fig. 3A). The maintenance of *SCX* expression levels has

been also observed in our previous works [27]. Overall, IL-1β treatment combined with PEMF stimulation leads to an increment in tendon gene expression up to the levels of non-IL-1β magCSs (Control group).

The presence of the tenogenic proteins MKX and TNMD were also investigated. MKX and TNMD were observed in all conditions (Fig. 3B), however the signal intensity of MKX was lower in magCSs treated with IL-1β. Additionally, the presence of these proteins together with collagen III was confirmed by western blot analysis (Fig. 4Bii).

3.3. Tendon-like ECM matrix in magCSs

The normal function of tissues depends on the maintenance of the unique extracellular matrix (ECM) composition and architectural arrangements. In the particular case of tendon tissues, the matrix organization is critical to provide structure and biomechanical properties. Since we supplemented magCSs with a powerful inflammatory mediator that could contribute for architectural changes in ECM, we assessed the expression of enzymes associated to collagen degradation and to ECM remodeling phenomena.

As expected, the expression of *MMP-1*, *MMP-2* and *MMP-3* increased with IL-1β treatment in comparison to control group (*MMP-1*, $p<0.01$; *MMP-2*, *MMP-3* $p<0.0001$) and to magCSs exposed to PEMF (*MMP-1*, $p<0.05$; *MMP-2*, *MMP-3*, $p<0.0001$) (Fig. 4Ai) [17, 27]. Interestingly MMP-1 and MMP-3 levels in IL-1β-magCSs stimulated with PEMF are higher than in control group (*MMP-1*, $p<0.01$; *MMP-3*, $P<0.0001$). Also, the expression of *TIMP-1* is upregulated in magCSs stimulated with PEMF ($p<0.0001$), while in IL-1β-magCSs was downregulated ($p<0.0001$, in comparison to non-PEMF IL-1β-magCSs) (Fig. 4Aii). It has been reported that increased levels of MMPs and low levels of TIMP-1 are associated to the degenerative changes in chronic tendinopathy [29]. In inflammatory conditions, elevated

MMPs and decreased expression of inhibitors result in the degradation of collagens, proteoglycans and elastin fibers in the ECM [30].

In sum, the IL-1β-magCSs respond to IL-1β supplementation at the gene expression level. PEMF seems to stimulate positively the expression of *MKX*, *TNMD*, *DCN* and *TIMP-1*, and inhibit *MMP-1*, *MMP-2* and *MMP-3* in IL-1β-magCSs.

Collagen type I is the major protein in connective tissues and an increase in collagen type III has been related both to remodeling phase of healing and to fibrotic tissues [31]. We further investigated how IL-1β treatment could directly affect the degradation of collagen and other proteins in ECM produced by magCSs. The expression of collagen type I (*COL1A1)* was decreased in IL-1β-magCSs ($p<0.0001$ in comparison to control group) but collagen type III (*COL3A1)* remained unchanged ($p>0.05$) (Fig. 4Aiii).

However, in terms of collagen production, no significant differences were found between control and IL-1β-magCSs groups ($p>0.05$). Nevertheless, the production of non-collagenous proteins was deeply reduced in IL-1β-magCSs ($p<0.0001$ in comparison to Control group and to IL-1β-magCSs stimulated with PEMF group) (Fig. 4Bi).

When PEMF is applied on IL-1β-magCSs, there is an increment in the *COL3A1* expression ($p<0.001$) and in the amount of both collagenous ($p<0.0001$) and non-collagenous ($p<0.0001$) proteins. The increment is also significant in comparison to magCSs Control group ($p<0.0001$) (Fig. 4Bi), suggesting an anabolic role of PEMF in magCSs treated with IL-1β on the quality and quantity of the ECM.

Thus, PEMF seems to significantly influence the production of collagen ($p<0.05$) in IL-1β-magCSs. The fact that collagen synthesis is also increased in comparison to control ($p<0.05$) group suggests that PEMF promotes the deposition of a collagen rich-ECM matrix. Furthermore, the increased levels of *COL3A1* also supports that the synthesis and deposition of collagen type I and collagen type III, necessary for the remodeling process [32].

3.4. Investigation of cytokine profile in magCSs

In an inflammatory milieu, cells communicate through networks of inflammatory mediators to inform about extracellular conditions and adjust the response accordingly. The treatment of magCSs with IL-1β was aimed to study tendon cell responses to such cues in a cellular matrix enabling juxtacrine and paracrine signaling. Pro-inflammatory genes *IL-8*, *IL-1β*, *TNFα*, and *IL-6* showed increased expression in IL-1β-magCSs, when compared with the other groups under study ($p<0.05$) (Fig. 5Ai). Furthermore, the transcript levels of anti-inflammatory factors *IL-10 and IL-4* were decreased in IL-1β-magCSs, in comparison to control (*IL-10*, $p<0.05$; *IL-4*, $p<0.01$) and to PEMF stimulated (*IL-10*, $p<0.0001$; *IL-4*, $p<0.0001$) conditions (Fig. 5Bi).

These results are supported by ELISA assays, which showed higher concentrations of TNFα and IL-6 but lower amounts of IL-10 released by IL-1β-magCSs (TNFα, $p<0.05$; IL-6, $p<0.0001$ in comparison to Control group). The effect of PEMF on the inflammatory profile of IL-1β-magCSs was also investigated (Fig. 5B). PEMF stimulation caused a decrease in the genetic expression of pro-inflammatory cytokines and an increase in the expression of anti-inflammatory associated genes (*IL-8*, $p<0.001$; *IL-1β*, $p<0.05$; *TNFα*, $p<0.001$; IL-6, $p<0.0001$ in comparison to IL-1β-magCSs). Interestingly, the *TNFα* showed levels of expression even lower than the Control group ($p<0.05$), while the expression of both *IL-4 and IL-10* was approximately 3-fold higher ($p<0.05$) (Fig. 5Bi). The dissimilar values between PEMF and Control groups may be associated to the anti-inflammatory effect of PEMF, even in the absence of IL-1β treatment.

Correlating with the results obtained for gene expression, the release into the culture medium of TNFα and IL-6 were significantly reduced under PEMF in comparison to IL-1β-magCSs ($p<0.0001$) and to the Control group ($p<0.01$) (Fig. 5Aii). The concentration of PGE_2, a lipid

mediator of pain and acute inflammation, also followed this trend (IL-1β-magCSs, $p<0.001$; magCSs Control, $p<0.05$) (Fig. 5Aii).

Additionally, the release of IL-10, was significantly increased with PEMF in comparison to the other conditions (Control group, $p<0.01$; IL-1β-magCSs, $p<0.0001$) (Fig. 5Bii). As expected, tendon cells in magCSs constructions respond to IL-1β treatment with pronounced pro-inflammatory cues. Moreover, the pro-inflammatory signals can be modulated by exposure to PEMF, as observed in IL-1β-magCSs, in which the expression levels of pro-inflammatory cues were lower than the ones shown for other conditions. According to these outcomes, PEMF seems to effectively reestablish the levels of anti-inflammatory factors in inflammatory conditions, necessary to the resolution of inflammation to continue healing.

3.5. Involvement of MAPK signaling pathway in the regulation of inflammation cues

In the complex inflammation process, different signaling pathways may be involved and may contribute to the activation and production of multiple pro-inflammatory molecules, namely IL-1β, TNFα or IL-6 [32-34]. The p38 mitogen associated protein kinase MAPK(ER1/2) pathway is involved in many tissues responses, including tendons tissues. [35-37]. In this sense, and considering the gene and protein response of magCSs to IL-1β treatment concomitantly modulated by PEMF stimulation, we investigated the potential of MAPK/ERK1/2 on magCSs regulation (Fig. 6). The MAPK(ER1/2) activation is a consequence of different cytokine stimuli, including IL-1β, triggering the expression of pro-inflammatory factors, such as COX-2 and PGE_2 [38].

The results of phospho-MAPK(ERK1/2) were assessed by western blot (Fig. 6Ai). Although the bands do not show evident differences, the quantification of the bands intensity indicates that PEMF reduces phospho-MAPK(ERK1/2) in magCSs. Phosphorylated ERK1/2 was further assessed by ELISA assays and follow the trend of the cytokine profile, with an increased concentration in IL-1β-magCSs (Control group, $p<0.05$) (Fig. 6Aii). Again, PEMF

stimulated IL-1β-magCSs show lower values in comparison to control group ($p<0.001$) (Fig. 6Ai). These results can suggest a possible role and targeted action of PEMF in MAPK(ERK1/2) activation in an IL-1β induced pro-inflammatory response.

The pro-inflammatory factors, COX-2 and PGE_2, have been widely described as products resultant from MAPK pathway activation [37-39] (Fig. 6B). In this study, both *COX-2* transcripts and protein expression were increased with IL-1β treatment ($p<0.05$), and decreased with PEMF stimulation ($p<0.05$) (Fig. 6Bi).

The release of PGE_2 demonstrates a similar tendency (Fig. 6Bii). Interestingly, under PEMF the amounts of released PGE_2 are lower than the ones of Control group ($p<0.05$).

4. Discussion

- **Establishment of an *in vitro* model with magCSs**

The prolonged exposure to pro-inflammatory mediators is known to lead to chronic inflammation [40], and ultimately to tendon disorders. Exposing magnetic tendon cell sheets to an inflammatory cytokine-rich milieu, we expected to more accurately predict tendon cell behavior *in vivo* and the potential immunomodulatory contributions of magCSs for tendon therapies.

To antagonize such influence and improve scaffold-free strategies, we also explored the immunomodulatory effect of PEMF on magCSs conditioned to IL-1β.

The inflammatory stimulus provided by IL-1β influenced the tenogenic phenotype reducing the relative gene expression of *MKX, TNMD,* and *DCN*. Conversely, pro-inflammatory genes were increased, supported by the increment of pro-inflammatory mediators secreted by IL-1β-magCSs. These outcomes, together with the decrease in anti-inflammatory genes and soluble factors, IL-4 and IL-10, suggest that magCSs respond to IL-1β by increasing the expression and production of inflammatory factors into the environment[41, 42]. This

response also resulted in a decrease in *COL1A1* expression and in the synthesis of ECM proteins (non-collagenous) suggesting that inflammatory stimuli may also interfere with the quality of the ECM. The matrix composition, organization and cell-matrix interactions are important for normal function of tendon. However, during tendinopathy conditions the normal composition of ECM suffers alterations and has been suggested to be the major factor for the development of this disorder [32]. These alterations interfere with the inflammatory cell signaling and with the cytokine release, thus affecting the important mechanisms of repair [43]. These mediators are responsible for ECM disorganization, which was recognized as a major cause for tendon injuries. In tendinopathy conditions, matrix degradation and the collagen content becomes more heterogeneous and disordered [31, 44]. The degradation of collagen is normally regulated by MMPs and by the activity of their inhibitors (TIMPs). Miller et al.[45] reported that pro-inflammatory factors as TNFα and IL-1α stimulate catabolic degradation of collagen matrix via MMP-2 in intervertebral disc cells under normal and inflammatory environments, stimulated by IL-1α.

To elucidate on the mechanisms associated to the IL-1β treatment, we investigated a possible involvement of the intracellular signaling pathway, MAPK(ERK1/2), which is activated by stressful and pro-inflammatory stimuli.

Our results indicated that IL-1β treatment leads to the activation of MAPK(ERK1/2), likely due to the increment in IL-1β expression on magCSs. In addition, results demonstrated higher expressions of COX-2 and PGE_2 by the IL-1β-magCSs. COX-2 is responsible for the high levels of prostaglandins, such as PGE_2 present in acute and chronic inflammation. MAPK (ERK1/2) signaling is involved in COX-2 expression and the inhibition of this pathway causes a reduced COX-2 expression [46]. Moreover, several studies focusing on inflammation reported that IL-1β influences the levels of COX-2 and PGE_2 through the activation of the MAPK(ERK1/2) pathway [39, 43-45, 47].

- **Contributions of PEMF stimulation to resolve inflammatory cues in IL-1β-magCSs**

From our previous studies, PEMF has shown a great impact in the inflammatory profile of IL-1β-hTDCs influencing the release and expression of cytokines [17, 18, 39]. Despite the fact that such works were performed in monolayer cultures and in the absence of MNPs, the combination of MNPs actuated by an external magnetic field could stimulates specific biochemical responses [48]. The response of MNPs to magnetic fields can provide additional signals that cells respond to, likely creating synergistic actions to guide the healing process [2]. For instance, the combination of MNPs and scaffolds with magnetic fields and stem cells has shown to increase the osteogenic differentiation, angiogenesis and bone regeneration [49]. Moreover, cell internalized MNPs can be visualized by conventional imaging techniques (e.g. MRI, CT), enabling visualization in preclinical and clinical approaches.

We investigated a possible influence of MNPs and PEMF on cell organization and distribution within magCSs. The results showed a tendency for parallel alignment of tendon cells, within magCSs constructions. The cellular organization is an important point to obtain proper healing and disorganized architectures may favor degenerative conditions mediated by pro-inflammatory niches [44].

In relation to gene expression level, magnetic stimulation in inflamed environment provoked a pronounced increase in *MKX*, *TNMD* and *DCN*. Herein, the expression of genes encoding for matrix degrading enzymes were downregulated after the exposure to PEMF, and upregulated for the *TIMP-1* in comparison to the Control group.

Moreover, the expression of collagens increased in IL-1β-magCSs under PEMF stimulation and consequently the production of collagen proteins. During the healing process, high production of collagen fibers is essential, where collagen type III is required for the assemble

of collagen type I fibers. Thus, an increase in collagen type III may suggest cellular guidance towards healing [31].

Our results demonstrate that PEMF supports the production of a tendon-like matrix, promote collagen synthesis, and a decrease in MMPs gene expression, evidencing a regulatory influence of PEMF in tendon healing process. Understanding the mechanisms associated to the expression of inflammatory mediators may provide molecular tools for improving current therapeutics [50]. The effect of PEMF in MAPK(ERK1/2) activation of IL-1β-magCSs and the consequent synthesis of COX-2 and PGE_2,was investigated in this work. Several studies have reported that PEMF can modulate the activation of intracellular signaling associated to inflammatory profiles mediated by NF-Kb, mTOR or MAPK pathways [17, 51]. Additionally, the phosphorylation of p38 MAPK(ERK1/2) was shown to be inhibited by the exposure to PEMF (1.5mT; 75Hz, 10% duty cycle) in an inflammatory model of synovitis, leading to the decrease of TNFα [52].

In our study, we demonstrate not only a reduction on the phosphorylation of MAPK(ERK1/2) in IL-1β-magCSs but also reduced levels of COX-2 and PGE_2. An exposure to a PEMF (1.5 mT, 75 Hz, 1/10 duty cycle) was also shown to reduce the release of PGE_2 as well as of IL-6 and IL-8 from bovine synovial fibroblasts from osteoarthritis patients treated with IL-1β [53]. Thus, the reduction on the phosphorylation of MAPK(ERK1/2) could also indicate that PEMF may influence the expression and synthesis of pro-inflammatory cytokines and lipid mediators COX-2 and PGE_2 in magCSs through MAPK(ERK1/2). These outcomes are in accordance with published studies[51] supporting the application of magnetic fields in pathologies with an inflammatory context.

Overall, these results show the applicability of magCSs as a cellular model for tendon studies. Moreover, PEMF shows a relevant influence over inflammatory mediators and in the quality

and quantity of ECM in magCSs that goes beyond the expression of cytokines, and may depend on MAPK(ERK1/2) pathway.

5. Conclusions

This work shows that magCSs technologies offer new possibilities as advanced cell culture models for tendon tissue engineering, including pathophysiological models of inflammation to assist the understanding of the onset and progression of tendon disorders. In accordance to previous studies, PEMF evidences a modulatory action in the inflammatory profile of IL-1β primed tendon cells in magCSs constructions, via MAPK(ERK1/2) pathway. The remote control over magCSs strengthens the role of PEMF in tendon therapies, and highlights the promise of magCSs as a living patch to overcome sustained inflammatory events and to drive tendon repair and regeneration.

Conflict of interest

The authors declare no conflict of interest.

Data availability statement

The data that support the findings of this study are available from the corresponding author upon reasonable request.

Declaration of interests

☒ The authors declare that they have no known competing financial interests or personal relationships that could have appeared to influence the work reported in this paper.

Statement of significance

The combination of cell sheets and magnetic-based technologies holds promise as instrumental bio-instructive tools both for tendon disease modelling and for the development of magnetically responsive living tendon substitutes.

We have previously shown that remote actuation of a pulsed electromagnetic field (PEMF) modulated the inflammatory response of IL-1β-treated human tendon-derived cell (hTDCs) monolayers. As magnetic cell sheets (magCSs) technologies enable improved cellular organization and matrix deposition, these constructions could better recapitulate tendon niches. In this work, we aimed to apply magCSs technologies to study hTDCs responses in inflammatory environments. Overall results show that PEMF-stimulated-magCSs hold evidence for immunomodulatory properties and to become a living tendon model envisioning tendon regenerative therapies.

Acknowledgements

This research was funded by the ERC CoG MagTendon (No. 772817), Fundação para a Ciência e Tecnologia (FCT) for the doctoral grant PD/BD/128089/2016 of A. Vinhas and the project MagTT PTDC/CTM-CTM/29930/2017 (POCI-01-0145-FEDER-29930), project Norte-01-0145-FEDER-02219015 supported by Norte Portugal Regional Operational Programme (NORTE 2020) and EC Twinning project Achilles (No. 810850). The authors thank Hospital da Prelada (Porto, Portugal) for providing tendon samples.

References

[1] D. Cigognini, A. Lomas, P. Kumar, A. Satyam, A. English, A. Azeem, A. Pandit, D. Zeugolis, Engineering in vitro microenvironments for cell based therapies and drug discovery, Drug Discov Today 18(21-22) (2013) 1099-108.

[2] A.I. Gonçalves, M.T. Rodrigues, M.E. Gomes, Tissue-engineered magnetic cell sheet patches for advanced strategies in tendon regeneration, Acta biomaterialia 63 (2017) 110-122.

[3] Y. Lu, W. Zhang, J. Wang, G. Yang, S. Yin, T. Tang, C. Yu, X. Jiang, Recent advances in cell sheet technology for bone and cartilage regeneration: from preparation to application, Int J Oral Sci 11(2) (2019) 17.

[4] M. Li, J. Ma, Y. Gao, L. Yang, Cell sheet technology: a promising strategy in regenerative medicine, Cytotherapy 21(1) (2019) 3-16.

[5] Y. Qi, W. Yan, Mesenchymal stem cell sheet encapsulated cartilage debris provides great potential for cartilage defects repair in osteoarthritis, Med Hypotheses 79(3) (2012) 420-1.

[6] H. Shen, R. Jayaram, S. Yoneda, S.W. Linderman, S.E. Sakiyama-Elbert, Y. Xia, R.H. Gelberman, S. Thomopoulos, The effect of adipose-derived stem cell sheets and CTGF on early flexor tendon healing in a canine model, Sci Rep 8(1) (2018) 11078.

[7] A. Ito, M. Hayashida, H. Honda, K. Hata, H. Kagami, M. Ueda, T. Kobayashi, Construction and Harvest of Multilayered Keratinocyte Sheets Using Magnetite Nanoparticles and Magnetic Force, Tissue Engineering 10(5(6)) (2004) 873-880.

[8] A.I. Goncalves, M.S. Miranda, M.T. Rodrigues, R.L. Reis, M.E. Gomes, Magnetic responsive cell-based strategies for diagnostics and therapeutics, Biomed Mater 13(5) (2018) 054001.

[9] H. Akiyama, A. Ito, Y. Kawabe, M. Kamihira, Genetically engineered angiogenic cell sheets using magnetic force-based gene delivery and tissue fabrication techniques, Biomaterials 31(6) (2010) 1251-9.

[10] M. Ishii, R. Shibata, Y. Numaguchi, T. Kito, H. Suzuki, K. Shimizu, A. Ito, H. Honda, T. Murohara, Enhanced angiogenesis by transplantation of mesenchymal stem cell sheet created by a novel magnetic tissue engineering method, Arterioscler Thromb Vasc Biol 31(10) (2011) 2210-5.

[11] H. Akiyama, A. Ito, M. Sato, Y. Kawabe, M. Kamihira, Construction of cardiac tissue rings using a magnetic tissue fabrication technique, Int J Mol Sci 11(8) (2010) 2910-20.

[12] K. Shimizu, A. Ito, T. Yoshida, Y. Yamada, M. Ueda, H. Honda, Bone tissue engineering with human mesenchymal stem cell sheets constructed using magnetite nanoparticles and magnetic force, J Biomed Mater Res B Appl Biomater 82(2) (2007) 471-80.

[13] Y. Yamamoto, A. Ito, M. Kato, Y. Kawabe, K. Shimizu, H. Fujita, E. Nagamori, M. Kamihira, Preparation of artificial skeletal muscle tissues by a magnetic force-based tissue engineering technique, Journal of Bioscience and Bioengineering 108(6) (2009) 538-543.

[14] C. Tang, Y. Chen, J. Huang, K. Zhao, X. Chen, Z. Yin, B.C. Heng, W. Chen, W. Shen, The roles of inflammatory mediators and immunocytes in tendinopathy, J Orthop Translat 14 (2018) 23-33.

[15] K. Ren, R. Torres, Role of interleukin-1beta during pain and inflammation, Brain Res Rev 60(1) (2009) 57-64.

[16] C.A. Dinarello, Interleukin-1 in the pathogenesis and treatment of inflammatory diseases, Blood 117(14) (2011) 3720-32.

[17] A. Vinhas, M.T. Rodrigues, A.I. Goncalves, R.L. Reis, M.E. Gomes, Pulsed Electromagnetic Field Modulates Tendon Cells Response in IL-1beta-Conditioned Environment, J Orthop Res 38(1) (2019) 160-172.

[18] A. Vinhas, A.F. Almeida, A.I. Goncalves, M.T. Rodrigues, M.E. Gomes, Magnetic Stimulation Drives Macrophage Polarization in Cell to-Cell Communication with IL-1beta Primed Tendon Cells, Int J Mol Sci 21(15) (2020).

[19] R. Gehwolf, B. Schwemberger, M. Jessen, S. Korntner, A. Wagner, C. Lehner, N. Weissenbacher, H. Tempfer, A. Traweger, Global Responses of Il-1beta-Primed 3D Tendon Constructs to Treatment with Pulsed Electromagnetic Fields, Cells 8(5) (2019).

[20] L. de Girolamo, D. Stanco, E. Galliera, M. Vigano, A. Colombini, S. Setti, E. Vianello, M.M. Corsi Romanelli, V. Sansone, Low frequency pulsed electromagnetic field affects proliferation, tissue-specific gene expression, and cytokines release of human tendon cells, Cell Biochem Biophys 66(3) (2013) 697-708.

[21] C.L. Ross, B.S. Harrison, Effect of pulsed electromagnetic field on inflammatory pathway markers in RAW 264.7 murine macrophages, J Inflamm Res 6 (2013) 45-51.

[22] M. Nardoni, E. Della Valle, M. Liberti, M. Relucenti, M.A. Casadei, P. Paolicelli, F. Apollonio, S. Petralito, Can Pulsed Electromagnetic Fields Trigger On-Demand Drug Release from High-Tm Magnetoliposomes?, Nanomaterials (Basel) 8(4) (2018).

[23] G. Rahmi, L. Pidial, A.K. Silva, E. Blondiaux, B. Meresse, F. Gazeau, G. Autret, D. Balvay, C.A. Cuenod, S. Perretta, B. Tavitian, C. Wilhelm, C. Cellier, O. Clement, Designing 3D Mesenchymal Stem Cell Sheets Merging Magnetic and Fluorescent Features: When Cell Sheet Technology Meets Image-Guided Cell Therapy, Theranostics 6(5) (2016) 739-51.

[24] A.I. Gonçalves, R. Costa-Almeida, P. Gershovich, M.T. Rodrigues, R.L. Reis, M.E. Gomes, Cell-Based Approaches for Tendon Regeneration, in: M.E. Gomes, R.L. Reis, M.T.

Rodrigues (Eds.), Tendon Regeneration: Understanding tissue physiology and development to engineer functional substitutes, Elsevier2015, pp. 187-203.

[25] R. Costa-Almeida, L. Gasperini, J. Borges, P.S. Babo, M.T. Rodrigues, J.F. Mano, R.L. Reis, M.E. Gomes, Microengineered Multicomponent Hydrogel Fibers: Combining Polyelectrolyte Complexation and Microfluidics, Acs Biomater Sci Eng 3(7) (2017) 1322-1331.

[26] Y. Bi, D. Ehirchiou, T.M. Kilts, C.A. Inkson, M.C. Embree, W. Sonoyama, L. Li, A.I. Leet, B.M. Seo, L. Zhang, S. Shi, M.F. Young, Identification of tendon stem/progenitor cells and the role of the extracellular matrix in their niche, Nature medicine 13(10) (2007) 1219-27.

[27] A. Vinhas, M.T. Rodrigues, A.I. Gonçalves, R.L. Reis, M.E. Gomes, Magnetic responsive materials modulate the inflammatory profile of IL-1β conditioned tendon cells. , Acta Biomater. (2020).

[28] K. Zhang, S. Asai, B. Yu, M. Enomoto-Iwamoto, IL-1beta irreversibly inhibits tenogenic differentiation and alters metabolism in injured tendon-derived progenitor cells in vitro, Biochem Biophys Res Commun 463(4) (2015) 667-72.

[29] J.D. Rees, M. Stride, A. Scott, Tendons--time to revisit inflammation, Br J Sports Med 48(21) (2014) 1553-7.

[30] M. Raeeszadeh-Sarmazdeh, L.D. Do, B.G. Hritz, Metalloproteinases and Their Inhibitors: Potential for the Development of New Therapeutics, Cells 9(5) (2020).

[31] H.R. Screen, D.E. Berk, K.E. Kadler, F. Ramirez, M.F. Young, Tendon functional extracellular matrix, J Orthop Res 33(6) (2015) 793-9.

[32] K. Lipman, C. Wang, K. Ting, C. Soo, Z. Zheng, Tendinopathy: injury, repair, and current exploration, Drug Des Devel Ther 12 (2018) 591-603.

[33] L. Chen, H. Deng, H. Cui, J. Fang, Z. Zuo, J. Deng, Y. Li, X. Wang, L. Zhao, Inflammatory responses and inflammation-associated diseases in organs, Oncotraget 9 (2018) 7204-7218.

[34] A. Kulawik, R. Engesser, C. Ehlting, A. Raue, U. Albrecht, B. Hahn, W.D. Lehmann, M. Gaestel, U. Klingmuller, D. Haussinger, J. Timmer, J.G. Bode, IL-1beta-induced and p38(MAPK)-dependent activation of the mitogen-activated protein kinase-activated protein kinase 2 (MK2) in hepatocytes: Signal transduction with robust and concentration-independent signal amplification, J Biol Chem 292(15) (2017) 6291-6302.

[35] J.M. Wilde, J.P. Gumucio, J.A. Grekin, D.C. Sarver, A.C. Noah, D.G. Ruehlmann, M.E. Davis, A. Bedi, C.L. Mendias, Inhibition of p38 mitogen-activated protein kinase signaling reduces fibrosis and lipid accumulation after rotator cuff repair, J Shoulder Elbow Surg 25(9) (2016) 1501-8.

[36] T. Nishikai-Yan Shen, S. Kanazawa, M. Kado, K. Okada, L. Luo, A. Hayashi, H. Mizuno, R. Tanaka, Interleukin-6 stimulates Akt and p38 MAPK phosphorylation and fibroblast migration in non-diabetic but not diabetic mice, PLoS One 12(5) (2017) e0178232.

[37] W. Liu, S. Huang, Y. Li, Y. Li, D. Li, P. Wu, Q. Wang, X. Zheng, K. Zhang, Glycyrrhizic acid from licorice down-regulates inflammatory responses via blocking MAPK and PI3K/Akt-dependent NF-kappaB signalling pathways in TPA-induced skin inflammation, Medchemcomm 9(9) (2018) 1502-1510.

[38] E. Molina-Holgado, S. Ortiz, F. Molina-Holgado, C. Guaza, Induction of COX-2 and PGE2 biosynthesis by IL-1b is mediated by PKC and mitogen-activated protein kinases in murine astrocytes, British Journal of Pharmacology 131 (2000) 152-159.

[39] Q. Xia, Q. Hu, H. Wang, H. Yang, F. Gao, H. Ren, D. Chen, C. Fu, L. Zheng, X. Zhen, Z. Ying, G. Wang, Induction of COX-2-PGE2 synthesis by activation of the MAPK/ERK

pathway contributes to neuronal death triggered by TDP-43-depleted microglia, Cell Death Dis 6 (2015) e1702.

[40] M.A. Sugimoto, L.P. Sousa, V. Pinho, M. Perretti, M.M. Teixeira, Resolution of Inflammation: What Controls Its Onset?, Front Immunol 7 (2016) 160.

[41] N.L. Millar, G.A. Murrell, I.B. McInnes, Inflammatory mechanisms in tendinopathy - towards translation, Nat Rev Rheumatol 13(2) (2017) 110-122.

[42] W. Morita, S.G. Dakin, S.J.B. Snelling, A.J. Carr, Cytokines in tendon disease, Bone Joint Res 6(12) (2017) 656-664.

[43] F.G. Thankam, Z.K. Roesch, M.F. Dilisio, M.M. Radwan, A. Kovilam, R.M. Gross, D.K. Agrawal, Association of Inflammatory Responses and ECM Disorganization with HMGB1 Upregulation and NLRP3 Inflammasome Activation in the Injured Rotator Cuff Tendon, Sci Rep 8(1) (2018) 8918.

[44] A.D. Schoenenberger, J. Foolen, P. Moor, U. Silvan, J.G. Snedeker, Substrate fiber alignment mediates tendon cell response to inflammatory signaling, Acta Biomater 71 (2018) 306-317.

[45] S.L. Miller, D.G. Coughlin, E.I. Waldorff, J.T. Ryaby, J.C. Lotz, Pulsed electromagnetic field (PEMF) treatment reduces expression of genes associated with disc degeneration in human intervertebral disc cells, Spine J 16(6) (2016) 770-6.

[46] W. Cho, J. Choe, Prostaglandin E2 stimulates COX-2 expression via mitogen-activated protein kinase p38 but not ERK in human follicular dendritic cell-like cells, BMC Immunol 21(1) (2020) 20.

[47] S.J. Desai, B. Prickril, A. Rasooly, Mechanisms of Phytonutrient Modulation of Cyclooxygenase-2 (COX-2) and Inflammation Related to Cancer, Nutr Cancer 70(3) (2018) 350-375.

[48] J. Henstock, A. El Haj, Controlled mechanotransduction in therapeutic MSCs- can remotely controlled magnetic nanoparticles regenerate bones?, Future Medicine (2015).

[49] Y. Xia, J. Sun, L. Zhao, F. Zhang, X.J. Liang, Y. Guo, M.D. Weir, M.A. Reynolds, N. Gu, H.H.K. Xu, Magnetic field and nano-scaffolds with stem cells to enhance bone regeneration, Biomaterials 183 (2018) 151-170.

[50] J.D. O'Neil, A.J. Ammit, A.R. Clark, MAPK p38 regulates inflammatory gene expression via tristetraprolin: Doing good by stealth, Int J Biochem Cell Biol 94 (2018) 6-9.

[51] C.L. Ross, Y. Zhou, C.E. McCall, S. Soker, T.L. Criswell, The Use of Pulsed Electromagnetic Field to Modulate Inflammation and Improve Tissue Regeneration: A Review, Bioelectricity 1(4) (2019) 247-259.

[52] J. Ouyang, B. Zhang, L. Kuang, P. Yang, X. Du, H. Qi, N. Su, M. Jin, J. Yang, Y. Xie, Q. Tan, H. Chen, S. Chen, W. Jiang, M. Liu, X. Luo, M. He, Z. Ni, L. Chen, Pulsed Electromagnetic Field Inhibits Synovitis via Enhancing the Efferocytosis of Macrophages, Biomed Res Int 2020 (2020) 4307385.

[53] A. Ongaro, K. Varani, F.F. Masieri, A. Pellati, L. Massari, R. Cadossi, F. Vincenzi, P.A. Borea, M. Fini, A. Caruso, M. De Mattei, Electromagnetic fields (EMFs) and adenosine receptors modulate prostaglandin E(2) and cytokine release in human osteoarthritic synovial fibroblasts, J Cell Physiol 227(6) (2012) 2461-9.

Figure Captions

Figure 1: Characterization of tendon cells in monolayers (A) and in magnetic cell sheets construction (magCSs) (B) after 3 days in culture. Cellular distribution assessed by HE staining (**Ai, Bi**) of the tendon cells monolayer and magCSs (scale bar 2000μm). Matrix deposition (**Aii, Bii**) assessed by Sirius red/Fast green collagen staining and immunolocation of Collagen I (COL I) (green). Nuclei were counterstained with DAPI (blue) (x63, scale bar 50μm). Insets are representative images in lower amplification (x20, scale bar 100μm).

Figure 2: Viability, proliferation and morphology of tendon cells in magnetic cell sheets (magCSs) after 3 days in culture. Ai) Cell viability was determined by MTS assay. **Aii)** Live and dead staining for viable (green) and dead (red) cells (x20, scale bar 50μm, merged images). **Aiii)** Cell content determined by the PicoGreen assay**. Aiv)** Nuclei elongation ratio. W defines nuclei width whereas L defines nuclei lenght . Symbols denote statistical differences * for $p<0.05$; ** for $p<0.01$ and **** for $p<0.0001$. **B)** SEM micrographs analysis (x500, 50μm). Insets are representative images of magCSs in lower amplification (x150, 100μm). The graphs and the tables represent the atomic percentage (wt %) of carbon (C), oxygen (O) and iron (Fe) detected in the magCSs of the different experimental groups. Two different samples per condition were considered. The "IL-1β" condition refers to magCSs treated with IL-1β while "IL-1β PEMF" defines magCSs treated with IL-1β exposed to PEMF. Control group refers to magCSs in the absence of IL-1β and PEMF.

Figure 3: Assessment of the genetic expression and immune-location of tenogenic markers in magnetic cell sheets (magCSs) after 3 days in culture. A) Relative gene expression of Mohawk (*MKX*), Scleraxis (*SCX*), Tenomodulin (*TNMD*), Decorin (*DCN*) by real time RT-PCR. Expression of target genes was normalized against GAPDH housekeeping gene. Symbols denote statistical differences, * for $p<0.05$; ** for $p<0.01$ and **** for $p<0.0001$. **B)** Immunolocation of the tenogenic markers (green), Mohawk and Tenomodulin assessed at day 3 (x63, scale bar 50 μm). Nuclei were counterstained with DAPI (blue). The "IL-1β" condition refers to magCSs treated with IL-1β while "IL-1β PEMF" defines magCSs treated with IL-1β exposed to PEMF. Control group refers to magCSs in the absence of IL-1β and PEMF.

Figure 4: Extracellular matrix in magnetic cell sheets (magCSs) after 3 days in culture. Ai) Relative gene expression of metalloproteinases (MMPs); metalloproteinases-1, -2, -3 (*MMP-1, MMP-2, MMP-3*), **Aii)** tissue inhibitor metalloproteinase-1 (*TIMP-1*) and **Aiii)** collagen type I **(***COL1A1)* and collagen type III (*COL3A1)* by real time RT-PCR. **Bi)** Quantification of collagen and non-collagenous proteins by Sirius Red/Fast Green Collagen staining kit. **Bii)** Western blot of collagen III (COL III), tenomodulin (TNMD) and mohawk (MKX). Protein lysates were analyzed by probing for COL III, TNMD, MKX and α-smooth muscle actin (control) (two experimental replicates from two biological replicates). Symbols denote statistical differences * for $p<0.05$; ** for $p<0.01$; *** for $p<0.001$ and **** for $p<0.0001$. Expression of target genes was normalized against GAPDH housekeeping gene. The "IL-1β" condition refers to magCSs treated with IL-1β while "IL-1β PEMF" defines magCSs treated with IL-1β exposed to PEMF. Control group refers to magCSs in the absence of IL-1β and PEMF.

Figure 5: Determination of gene expression and release of pro- and anti-inflammatory factors in magnetic cell sheets (magCSs) after 3 days in culture. Ai) Gene expression of pro-inflammatory genes (*IL-8, IL-1β, TNFα* and *IL-6*) and **Bi**) **anti-inflammatory genes (***IL-10* and *IL-4)* by real time RT-PCR analysis. Expression of target genes was normalized against GAPDH housekeeping gene. **Aii, Bii)** Release of TNFα, IL-6, PGE_2 and IL-10 quantified in cultured medium by ELISA assays. Symbols denote statistical differences * for $p<0.05$; ** for $p<0.01$; *** for $p<0.001$ and **** for $p<0.0001$. The "IL-1β" condition refers to magCSs treated with IL-1β while "IL-1β PEMF" defines magCSs treated with IL-1β exposed to PEMF. Control group refers to magCSs in the absence of IL-1β and PEMF.

Figure 6: phosphorylated MAPK(ERK1/2) in magnetic cell sheets (magCSs) after 3 days in culture. Ai) Western blot of phosphorylated MAPK (pMAPK (Erk1/2). Bands intensity were quantified to α-smooth muscle actin (control) (two experimental replicates from two biological replicates) and **Aii)** Quantification of ERK1/2 (pT202/Y204) by ELISA assay **Bi)** Relative expression of *COX-2*, and **Bii)** Quantification of COX-2 release in cultured medium. Expression of target genes was normalized against GAPDH housekeeping gene. Symbols denote statistical differences * for $p<0.05$; ** for $p<0.01$; *** for $p<0.001$ and **** for $p<0.0001$. The "IL-1β" condition refers to magCSs treated with IL-1β while "IL-1β PEMF" defines magCSs treated with IL-1β exposed to PEMF. Control group refers to magCSs in the absence of IL-1β and PEMF.

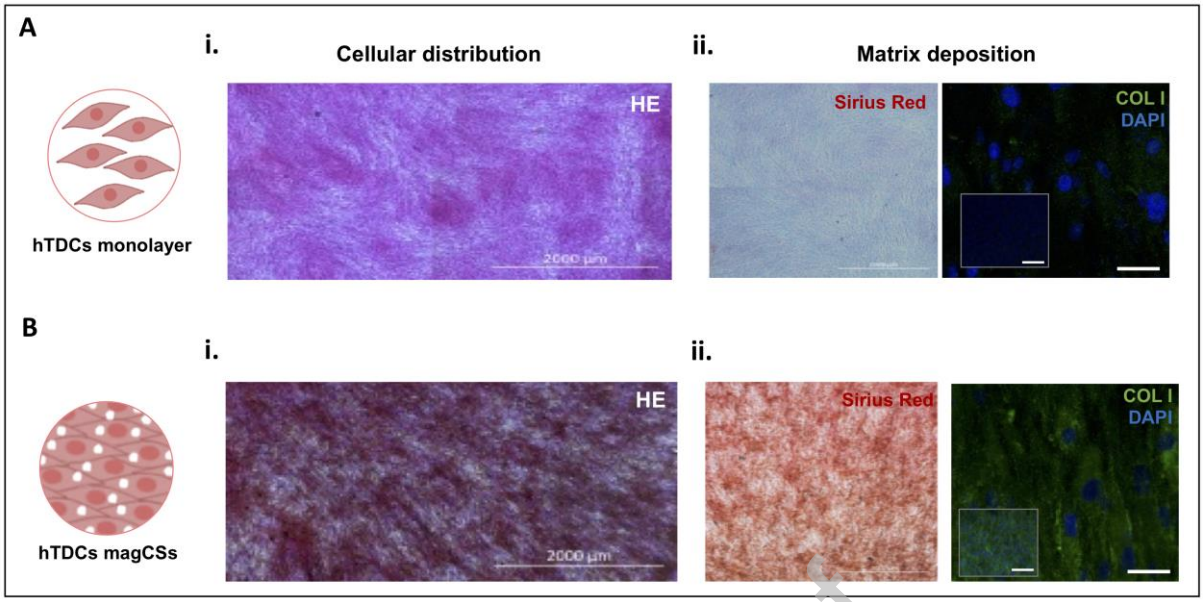

Fig. 1

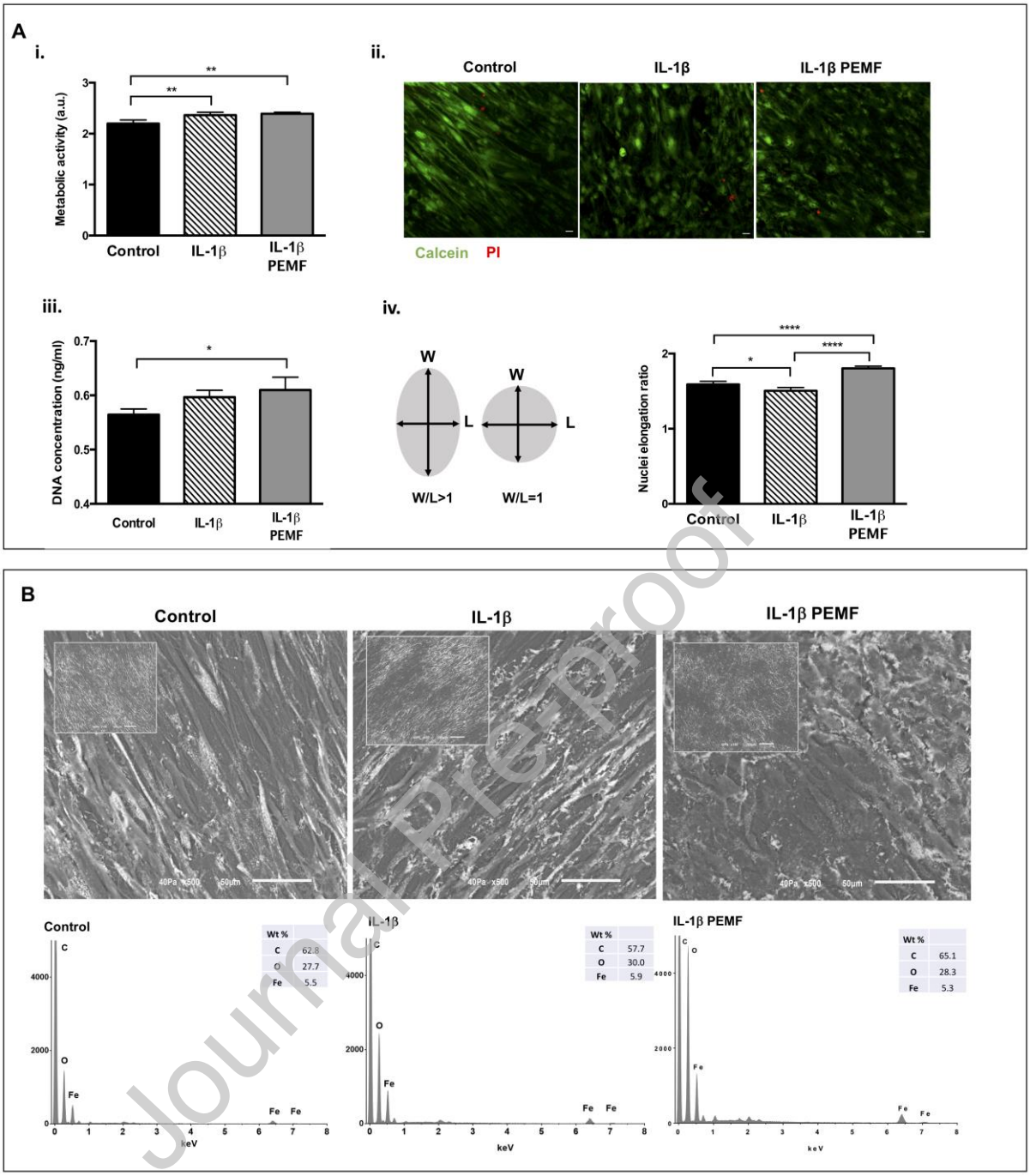

Fig. 2

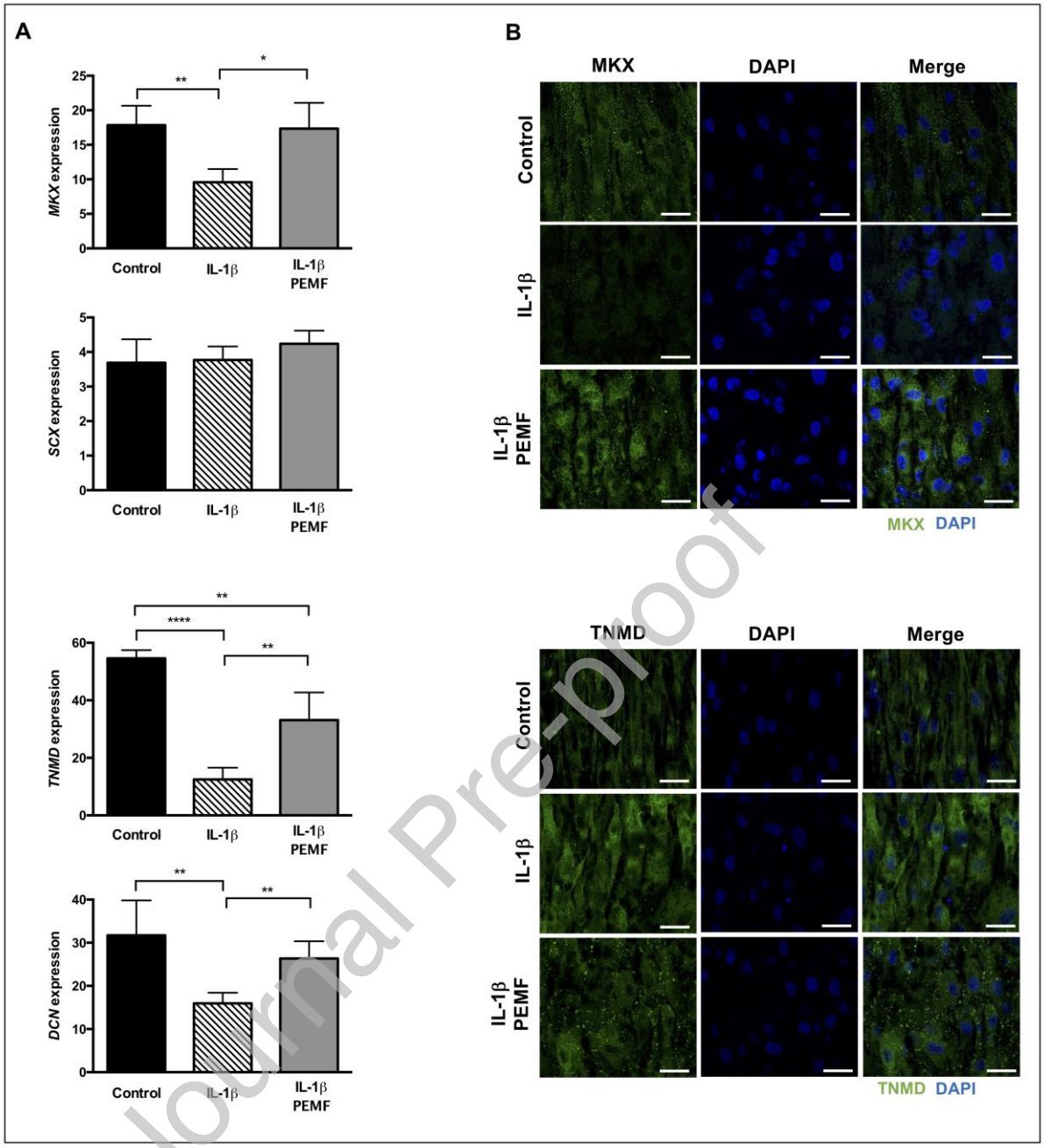

Fig. 3

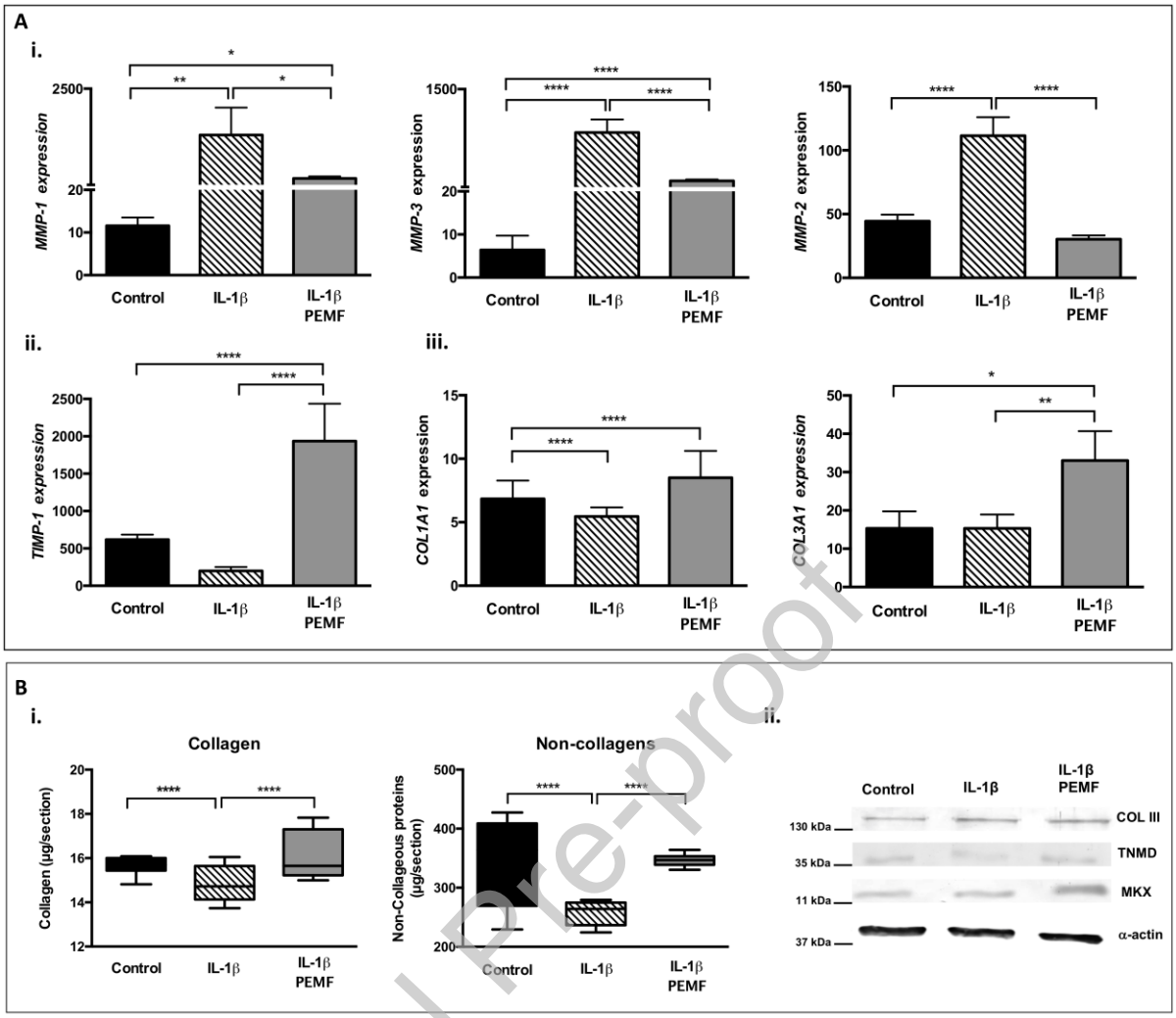

Fig. 4

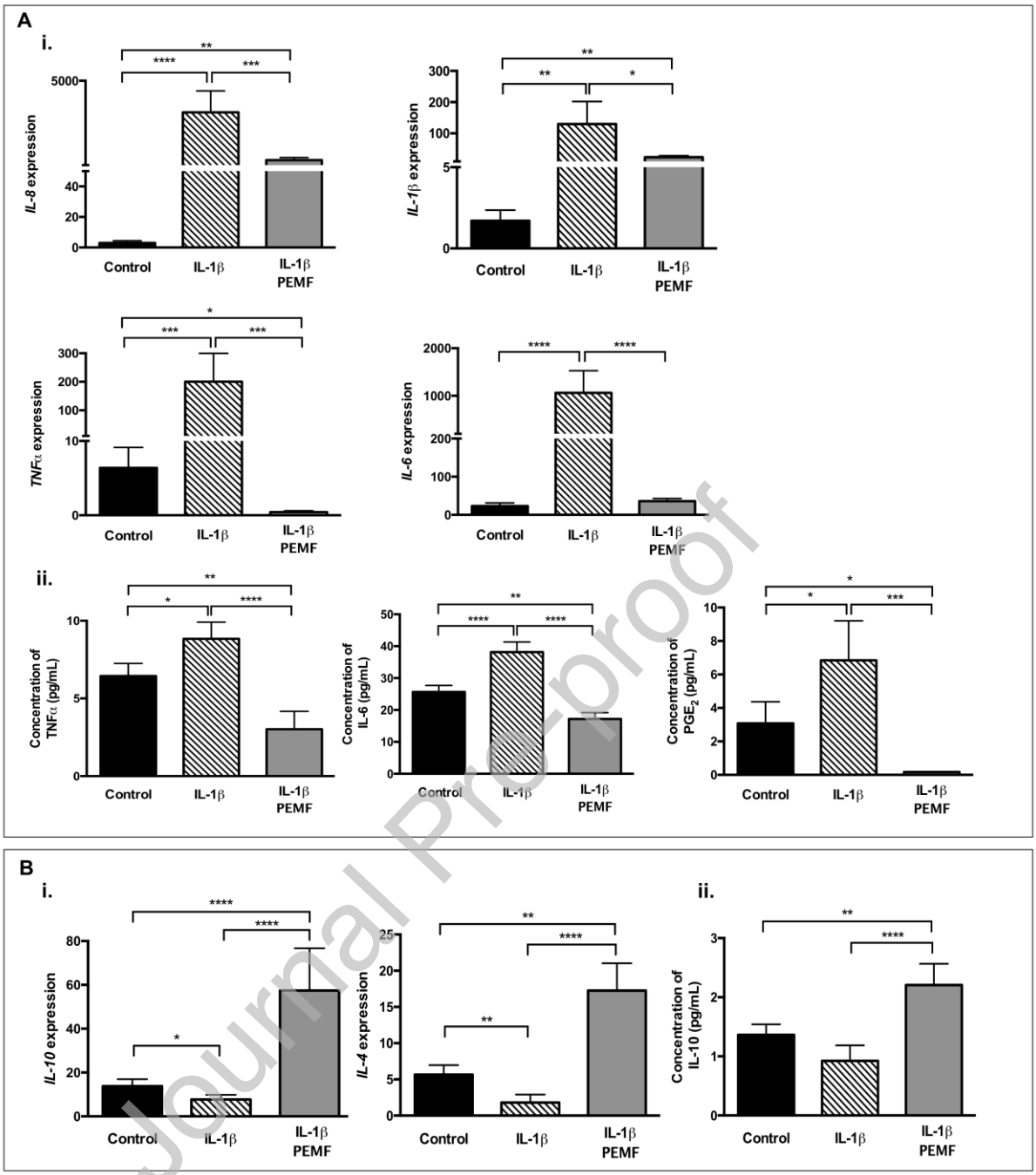

Fig .5

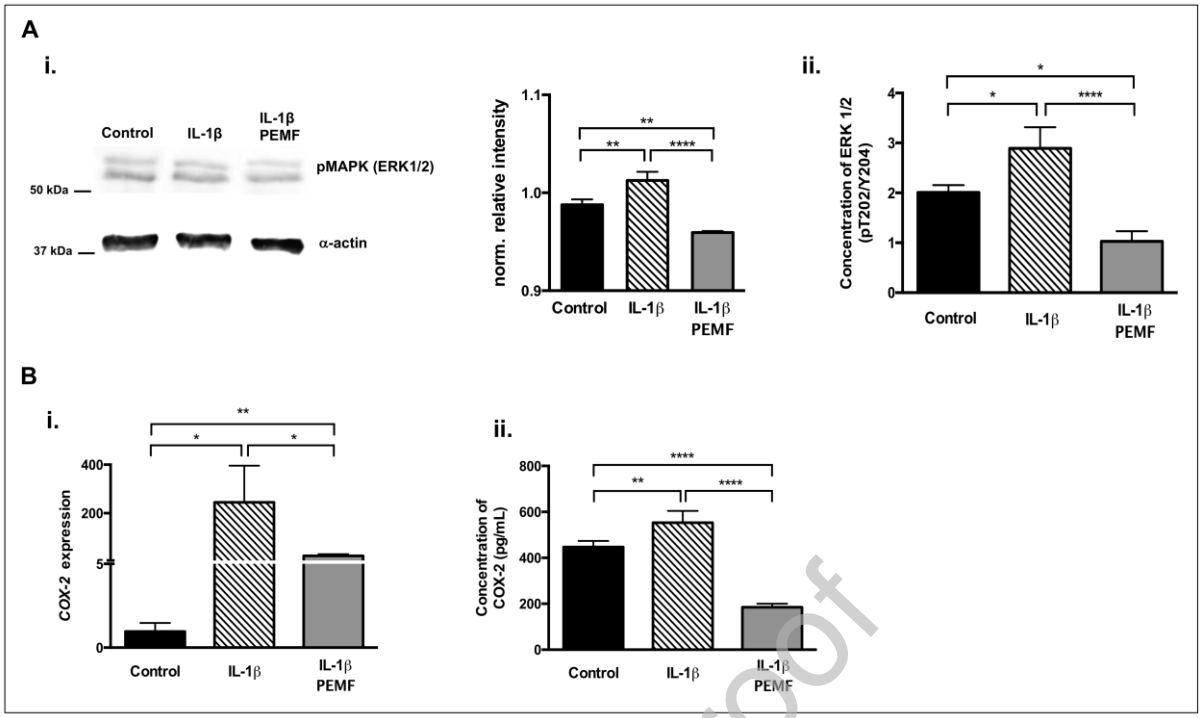

Fig. 6

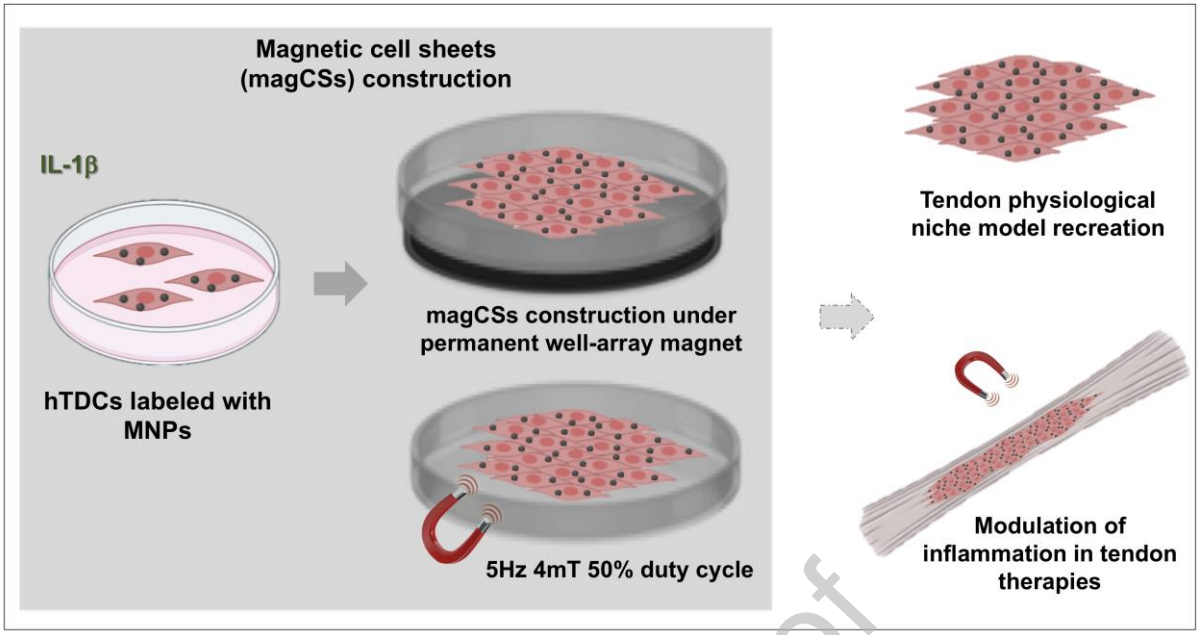

Graphical